Time-variable ice loss in Asian high mountains from satellite gravimetry

Koji Matsuo *, Kosuke Heki

Dept. of Natural History Sci., Hokkaido University, N10 W8, Kita-ku, Sapporo 060-0810, Japan

A R T I C L E   I N F O

A B S T R A C T

Substantial amount of glacial ice is considered to be melting in the Asian high mountains. Gravimetry by GRACE satellite during 2003–2009 suggests the average ice loss rate in this region of 47 ± 12 Gigaton (Gt) yr^{-1}, equivalent to ~0.13 ± 0.04 mm yr^{-1} sea level rise. This is twice as fast as the average rate over ~40 years before the studied period, and agrees with the global tendency of accelerating glacial loss. Such ice loss rate varies both in time and space; mass loss in Himalaya is slightly decelerating while those in northwestern glaciers show clear acceleration. Uncertainty still remains in the groundwater decline in northern India, and proportion of almost isostatic (e.g. tectonic uplift) and non-isostatic (e.g. glacial isostatic adjustment) portions in the current uplift rate of the Tibetan Plateau. If gravity increase associated with ongoing glacial isostatic adjustment partially canceled the negative gravity trend, the corrected ice loss rate could reach 61 Gt yr^{-1}.

© 2009 Elsevier B.V. All rights reserved.

1. Introduction

The extreme relief of Himalaya blocks the wet northward monsoon from the Indian Ocean that blows between June and September. The monsoon brings widespread and intense precipitation on the southern slopes of the range causing some of the highest total annual precipitation on the Earth. Such summer snows sustain mountain glaciers along the Himalayan high peaks. In the mountains to the northwest, e.g. Karakoram, winter snows fed by westerlies develop extensive mountain glaciers. These glaciers, together with those in mountain ranges to the north, e.g. Tien Shan and Pamir, form the largest store of water ice in the low and middle latitude region known as the "Third Pole" of the Earth (Qiu, 2008) (Fig. 1a).

The bulk of water ice on the Earth lies in continental ice sheets in Greenland and Antarctica. However, melting of smaller amount of mountain glaciers and ice caps is contributing more to the current eustatic sea level rise (Meier et al., 2007). Among these glaciers, more than a half of the total ice loss comes from those in southeastern Alaska, North America, high mountains (HM) in Asia, and Patagonia, South America (Kaser et al., 2006).

A system of twin satellites Gravity Recovery and Climate Experiment (GRACE), launched in 2002 to measure time-variable gravity field with monthly time resolution, enabled direct measurement of mass loss rates over extensive mountain glacier systems. GRACE observations in southeastern Alaska (Tamisiea et al., 2005; Chen et al., 2006) and Patagonia (Chen et al., 2007) provided independent supports for earlier topographic and altimetric estimates of ice loss rates there. Meier (1984) speculated

that rates of ice loss of glaciers due to global warming may scale with amplitudes of their seasonal volume changes. This rule of thumb holds true for the averages of ice loss rates during 1961–2003 based on field observations (Dyurgerov and Meier, 2005) (white circles in Fig. 2). The modern geodetic estimates over the last decade also obey this rule, but they show values approximately twice as fast as the 1961–2003 rates (blue and green circles in Fig. 2) suggesting that melting of mountain glaciers undergoes worldwide acceleration. Here we focus on HM Asia, and try to constrain current ice loss rate there with GRACE paying attention to interannual variability of the rate, vertical crustal movements in the Tibetan Plateau, and changes in groundwater level in northern India.

2. Estimation of ice loss rate from gravity changes

2.1. GRACE data

The Earth's gravity field is modeled as a combination of spherical harmonics. A monthly GRACE data set consists of the coefficients of the spherical harmonics (Stokes' coefficients) C_{nm} and S_{nm} with degree n and order m complete to 60. We have used 82 data sets of monthly gravity fields from GRACE (Level-2 data, Release 4) between 2002 April and 2009 April, from Center for Space Research, Univ. Texas. Monthly deviations of Stokes' coefficients can be converted to monthly changes in gravity anomaly Δg at latitude θ and longitude ϕ by

$$\Delta g(\theta, \phi) = \frac{GM}{R^2} \sum_{n=2}^{\infty} \sum_{m=0}^{n} (n-1)(\Delta C_{nm} \cos m\phi + \Delta S_{nm} \sin m\phi) P_{nm}(\sin\theta),$$

where R is the equatorial radius, G is the universal gravity constant, and M is the Earth's mass. $P_{nm}(\sin\theta)$ is the nth degree and mth order

* Corresponding author. Tel./fax: +81 11 706 3826.
  E-mail address: kouji-matsuo@mail.sci.hokudai.ac.jp (K. Matsuo).
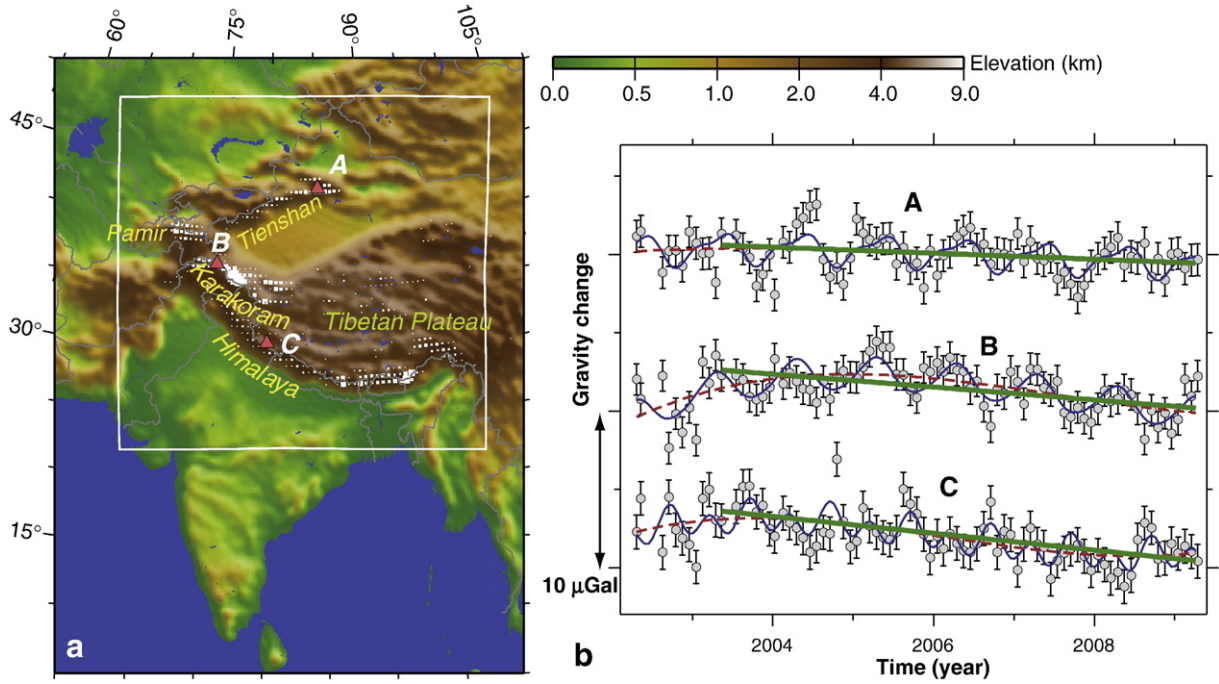
Fig. 1. (a) Distribution of glaciers (white dots) in Asian high mountains. (b) Gravity time series by GRACE at three points, A, B, and C, shown by red triangles in (a). Blue curves show best-fit models with polynomials with degrees up to three and seasonal changes. One-σ error bars are given a-posteriori to bring chi-squares of post-fit residuals unity. The polynomial parts of the model are shown by red broken curves. Thick green lines show an average trend from 2003 May to 2009 April. Gravity changes within the white rectangle in (a) are shown in Figs. 3 and 4. (For interpretation of the references to colour in this figure legend, the reader is referred to the web version of this article.)
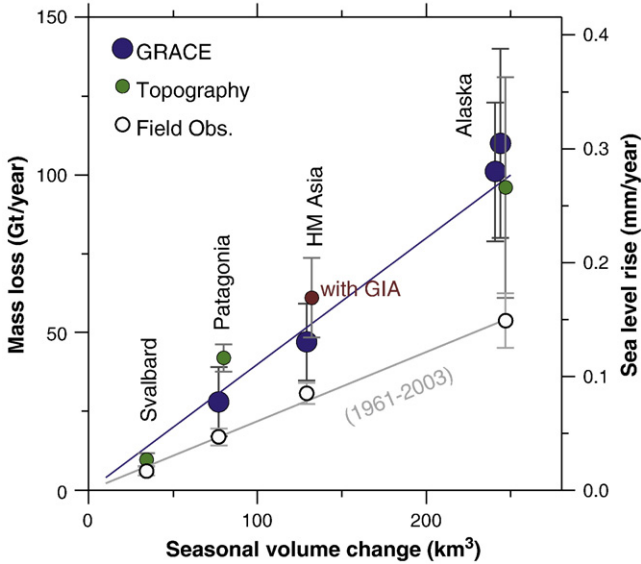

Fig. 2. Ice mass losses inferred from GRACE (blue), topography (green), and field observations (white), are shown against seasonal ice volume changes (Meier, 1984). If the TIBET-4 GIA model (Fig. 5b) were correct, the ice loss rate in HM Asia would be slightly larger (red circle). GRACE data cover 2002–2004 (Tamisiea et al., 2005), and 2002–2005 (Chen et al., 2006), for Alaska, 2002–2006 for Patagonia (Chen et al., 2007), and indicate value in 2003–2009 for HM Asia (this study). Topographic data cover 1995–2000 for Patagonia (Rignot et al., 2003), and from mid 1990s to 2000–2001 for Alaska (Arendt et al., 2002). In Svalbard, we multiplied 1.6, the ratio of the ice loss in 1996–2002 to those over the last 30–40 years (Bamber et al., 2005), with the 1961–2003 average ice loss rate. Average rates 1961–2003, shown by white circles, were inferred by compiling field observations of individual glaciers (Dyurgerov and Meier, 2005). The error bar for HM Asia is the combination of gravity time series fitting error (~7 Gt yr^{-1}), GLDAS land hydrological changes in the same period (~10 Gt yr^{-1}), and the difference in GIA models (~3 Gt yr^{-1}, only for the GIA corrected one). Actual numerical values are listed in Table S1. (For interpretation of the references to colour in this figure legend, the reader is referred to the web version of this article.)

fully-normalized Legendre function, and Δ indicates the deviation from the reference value. We also applied a Gaussian filter with averaging radius of 400 km to reduce short wavelength noise (Wahr et al., 1998), and replaced the Earth's oblateness values (C_{20}) with those from Satellite Laser Ranging (Cheng and Tapley, 2004). We also reduced longitudinal stripes with a filter proposed by Swenson and Wahr (2006), using polynomials of degree 5 for coefficients with orders 11 or higher. The movement of geocenter, expressed in the degree one component of the Stokes' coefficients, has not been considered. Gravity time series at three points in HM Asia are plotted in Fig. 1b.

We excluded data in the first year and obtained average trend over the six-year interval from 2003 May to 2009 April assuming seasonal (annual and semi-annual) and linear changes. The three points in Fig.1b all showed negative trends (green lines) suggesting that ice loss does occur in HM Asia. One sigma uncertainties of the trends are ~15% of the decrease rate on average, and this comprises a part of the estimation error of the current ice loss rate in HM Asia (Fig. 2). In order to interpret gravity changes in terms of surface mass variations, we calculate equivalent water thickness σ using the relationship (Wahr et al., 1998)

$$\Delta\sigma(\theta,\phi) = \frac{R\rho_{ave}}{3} \sum_{n=2}^{\infty} \sum_{m=0}^{n} \frac{2n+1}{1+k_n}(\Delta C_{nm}\cos m\phi + \Delta S_{nm}\sin m\phi)P_{nm}(\sin\theta),$$

where ρ_{ave} is the mean density of the Earth, and the load Love numbers k_n is to account for Earth's elastic yielding effect under the mass load in question. We assumed that the GRACE gravity changes during 2003–2009 reflect those in surface loads (Chao (2005) showed that the inverse solution is unique in that case), and converted them into equivalent water thickness. Fig. 3b shows the geographical distribution of load changes in terms of equivalent water thickness in HM Asia.
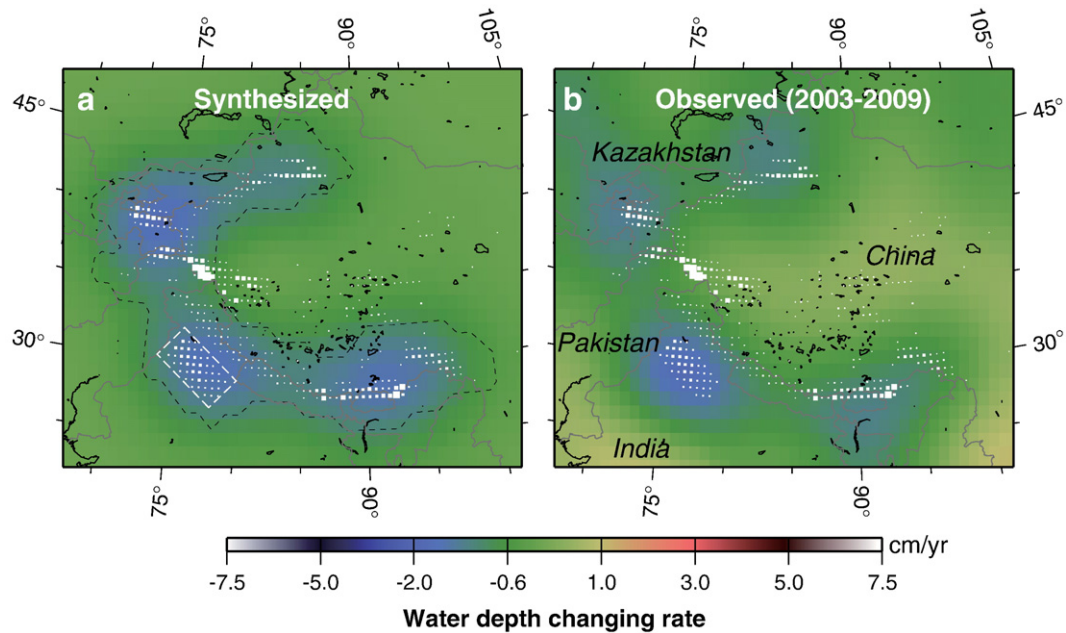
Fig. 3. Water level changing rates obtained by distributing 47 Gt yr^{-1} ice loss over HM Asia glaciers, and 10 Gt yr^{-1} ground water loss in northern Indian plain (white broken rectangle) (a). The average gravity decrease during 2003–2009 from GRACE, converted to equivalent water level changing rates after Wahr et al. (1998) (b). The same Gaussian spatial filter was applied in (a) and (b). Total mass loss was adjusted so that water decrease integrated over the area within the gray broken curve in (a) coincides between (a) and (b). (For interpretation of the references to colour in this figure legend, the reader is referred to the web version of this article.)

2.2. Estimation of ice loss rate

Total ice loss rate in HM Asia was inferred as follows, (i) assume a certain total mass loss rate and distribute it over the glaciers with prescribed geographical distribution, (ii) apply the same spatial filters as the GRACE data, (iii) repeat steps (i)–(ii) until the water decrease integrated over the region surrounding Asian HM glaciers (area within the broken curve in Fig. 3a) coincides between synthetic and observed data. The synthesized water level changes are shown in Fig. 3a.

In the step (i), we allocated the ice loss in proportion to the area covered by individual glacial regions (e.g. Himalaya, Hindukush, etc.) given in Dyurgerov and Meier (2005). There we applied some modifications, that is, we increased the weight of the two glacial regions, Tien Shan (× 1.5) and Pamir (× 2.0), to improve the correlation between the synthesized and the observed water change patterns. We assumed some mass increase for glaciers in Karakoram and Kunlun Shan to reproduce positive signals in the western part of the Tibetan Plateau.

In Fig. 3a we assumed the total ice loss rate of ~47 Gt yr^{-1} (blue dot in Fig. 2). This is much larger than the average during 1961–2003 (Dyurgerov and Meier, 2005) suggesting that similar acceleration to Alaska and Patagonia also occurred in HM Asia. This is not surprising considering that glaciers sustained by summer snows, such as those in Himalaya, are relatively sensitive to warming (Fujita and Ageta, 2000).

2.3. Spatio-temporal changes of the ice loss

In the gravity time series (Fig. 1b), we notice that actual variations are not linear. The red broken curves show non-seasonal part of the changes when we fit the whole data using a model with two additional terms proportional to t^2 and t^3 (t denotes time). They show different behaviors between points C and B. The former shows a relatively stable decrease and this trend slightly diminishes in the last part of the time series. The latter, in contrast, starts with an increase, and shows a decreasing trend only in the second half of the studied period. Fig. 4 shows maps of instantaneous water level changing rates at three epochs 2004.5, 2006.0, and 2007.5. There we see dramatic changes around the Pamir glacial system from the increase (Fig. 4a) to the rapid decrease (Fig. 4c).

In contrast to the Himalayan glaciers fed by summer monsoon, the western and northern glaciers such as in Pamir and Tien Shan get more precipitation from the westerly winds blowing between November and April. Field observations in 1997 and 2002 showed different behaviors of glaciers in these regions, that is, glaciers in Karakoram thickened while those in Himalaya generally thinned (Hewitt, 2005). This seems consistent with the spatio-temporal variability seen in the GRACE data (Fig. 4).

2.4. Land hydrology and anthropogenic groundwater loss in northern India

Natural changes in terrestrial water storage may obscure ice loss signals. Long-term land water storage trend is given by Global Land Data Assimilation System (GLDAS) (Rodell et al., 2004), and Fig. 5a shows the predicted water level change in the same time window as Fig. 3b (the same Gaussian filter has been applied to take account of the leakage from outside). We get negative changes of ~10 Gt yr^{-1} if we integrate such changes over the region within the broken curve in Fig. 3a. Reliability of long-term trends in GLDAS data is not well known. Here we do not correct the ice loss rate with this value, but let the error bar in Fig. 2 reflect it to show that this amount of uncertainty may exist.

Rapid increase of agricultural use of groundwater for crop irrigation has been posing a problem such as descent of groundwater level, drying of wells, and saltwater encroachments, in India. Such problems are serious in northern India; groundwater tables in the two states, Punjab and Haryana, show declining of 1–2 m yr^{-1} (Singh and Singh, 2002). This region (rectangle in Fig. 3a) is located within a few hundred kilometers from Himalaya, and the low spatial resolution of GRACE does not allow us to separate groundwater changes from glacial losses. Nevertheless, addition of sources of mass loss in the plain in northern India brings clear improvement in agreement of the synthesized and the observed changes (Fig. 3a,b). In that region we assumed groundwater loss in northern India as 10 Gt yr^{-1} (we exclude this amount when we discuss glacial losses). If this loss occurs uniformly over the entire two states, decrease of equivalent water depth amounts to ~0.1 m yr^{-1}. Water table declining due to overexploitation of groundwater is accelerating also in the Central
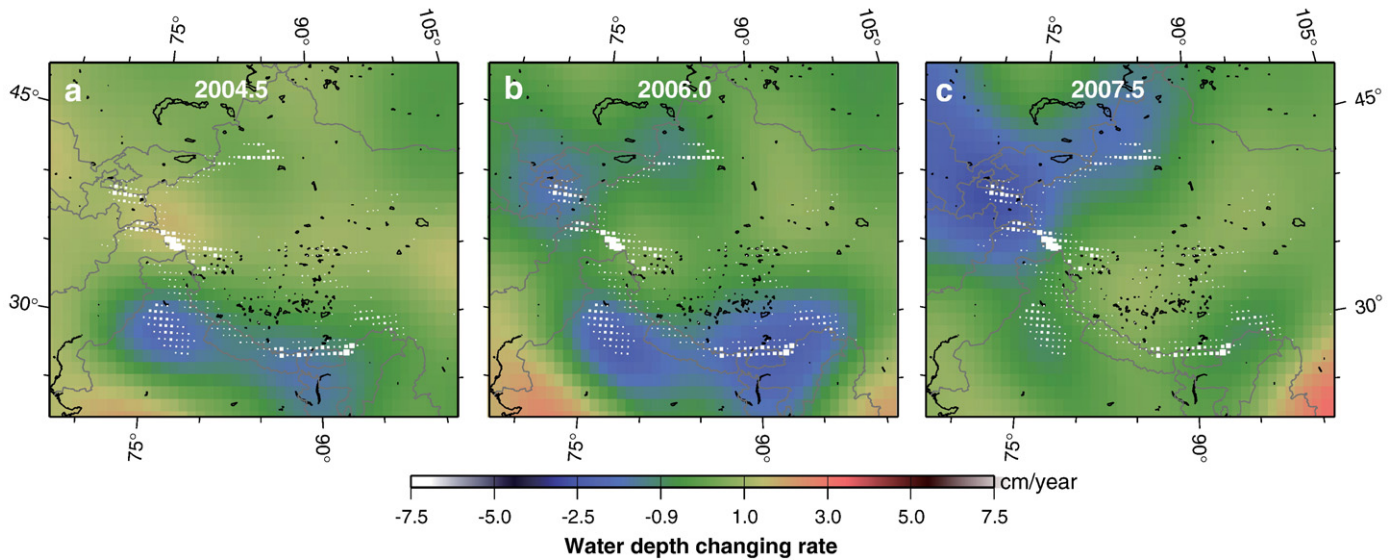
Fig. 4. Spatio-temporal variability of gravity changing rates expressed in equivalent water level changing rates at three epochs 2004.5 (a), 2006.0 (b) and 2007.5 (c).

Ganga Plain (Ahmed and Umar, 2008), and attention should be paid in future studies of time-variable gravity in Indian plains.

Concerning this issue, two new papers based on GRACE data analyses have been published. Rodell et al. (2009) suggested groundwater loss in northern India of 17.7 Gt yr^{-1}, over the states of Haryana, Punjab, and Rajasthan. Tiwari et al. (2009) estimated the total groundwater loss in the extensive region from northern to northeastern India as 54 Gt yr^{-1}. These values are larger than our assumption (10 Gt yr^{-1}), and might possibly include significant amount of glacial contributions. As mentioned already, without new gravimetry satellites with better spatial resolution (and without degrading temporal resolution), it is impossible to separate changes in northern Indian groundwater from glacial signals in this region.

3. Discussion

3.1. Gravity changes and uplift of the Tibetan Plateau

The Tibetan Plateau, known as the "roof of the world," has been formed by slow crustal uplift accumulated over a geological time scale. Recent studies of Tertiary paleo-altimetry suggested that the elevation of the Tibetan Plateau has been nearly constant for the last 15 Myr in the southern part (Spicer et al., 2003), and that the high altitude part has been growing progressively from south to north for the last 35 Myr (Rowley and Currie, 2006). Therefore the current tectonic uplift would not exceed a few mm yr^{-1} except in the northern Tibet and Himalaya, where relatively rapid tectonic uplift due to crustal thickening or convective removal of lithospheric mantle may still continue (Jiménez-Munt et al., 2008).

We should note that such tectonic uplifts are slow enough to go on without severely disturbing isostatic equilibrium. Even the recent uplift "pulse" of the southern Himalaya took 0.9 Myr (Amano and Taira, 1992), longer than time constants of typical GIA (Glacial Isostatic Adjustment) by two orders of magnitudes. Such uplifts would have been accompanied by denudation due to continuous erosion (Burbank et al., 1996). Because erosion is a result of the uplift, it would not go faster than the uplift. Therefore tectonic uplift and resultant denudation, even if they continue now, would make only small gravity changes. High degree of isostatic compensation is reflected in the deep crustal root beneath the plateau that keeps geoid
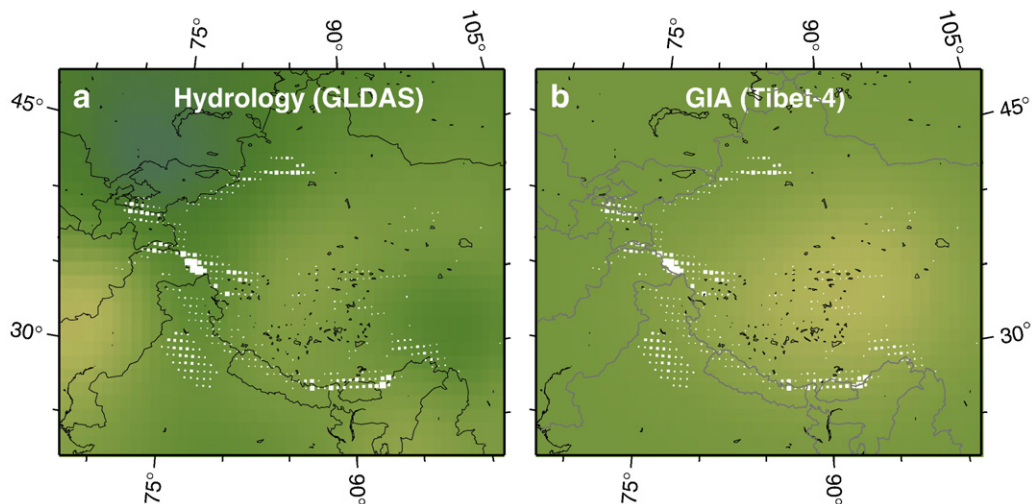

Fig. 5. The average water level changing rate during 2003–2009 by GLDAS land hydrology model (a), and gravity changing rates predicted by the TIBET-4 GIA model (Kaufmann, 2005) converted to apparent water level changes (b). The 400 km Gaussian filter is applied. The same color scheme as in Fig. 4 is used. (For interpretation of the references to colour in this figure legend, the reader is referred to the web version of this article.)

bump there as low as ~30 m (Jiménez-Munt et al., 2008). It would therefore require a long observing period and/or significant accuracy improvement to detect the present day geoid height change of tectonic origin with satellite gravimetry.

GIA is a slow uplift of the solid Earth as a delayed viscous response to past ice melting. It is accompanied with net increase of mass, which is often clearly observed with GRACE (Tamisiea et al., 2007). GIA causes underestimation of present day ice loss rate, and needs to be corrected if it exists (e.g. Chen et al., 2007). In the Tibetan Plateau, there are two distinct groups of models of ice sheet coverage in the Last Glacial Maximum, one assuming a large single ice sheet over the entire plateau and the other considering only a few small icecaps over high mountains (Kaufmann and Lambeck, 1997; Wang, 2001; Kaufmann, 2005). The large-GIA models predict ongoing uplift of the plateau detectable with Global Positioning System (GPS) observations.

3.2. Current uplift of the Tibetan Plateau from GPS

Horizontal crustal movements in the Central and Eastern Asia are well constrained by GPS observations (e.g. Wang et al., 2001), and Himalaya is known to show rapid uplift exceeding 5 mm/year (Bettinelli et al., 2006). However, vertical crustal movements within the Tibetan Plateau have been little documented and have large uncertainties (Xu et al., 2000). Lhasa (LHAS) is the only place, located within the plateau, with continuous GPS measurements of sufficient data length. Its uplift rates given in International Terrestrial Reference Frame (ITRF) 2000 and 2005 (Altamimi et al., 2007) are both less than 1 mm yr^{-1}. This contrasts with campaign GPS data in Tibet reporting uplift with average of 8 mm yr^{-1} over the plateau (Xu et al., 2000).

Fig. 6b–d shows residual (i.e. de-trended) time series of LHAS in ITRF2005 (Altamimi et al., 2007). Their data quality looks very different before and after a certain epoch ~2000.5, and clear seasonal

movements in up and north components are seen only after this epoch. Monsoon origin huge load south of Tibet, inferred from seasonal gravity changes (i.e. change in hydrological load) recovered by GRACE, depresses the ground and drags Tibet southward every summer (Fig. 6a). Such seasonal crustal movement can be calculated using seasonal changes of the Stokes' coefficients from GRACE data using load Love numbers h_n, l_n, and k_n (see Eq. (1) of Davis et al. (2004)).

Such seasonal displacement should repeat every year with similar signatures (Heki, 2001). Seasonal movement of Lhasa, however, obeys the predicted amplitude and phase only after 2000.5 (Fig. 6b–d). Whatever happened there in 2000, presence and absence of appropriate seasonal signatures suggest that only the second half of the data is trustable. The ~5.5 years of data after 2000.5 show uplift rate of 3.18 ± 0.13 mm yr^{-1}. Another GPS point (LHAZ) in Lhasa, with time span of ~2.3 years and proper seasonal signatures, shows uplift of 2.13 ± 0.56 mm yr^{-1}. Such uplifts are faster than the elastic rebound due to ice load removal by an order of magnitude (by doing the same calculation as the seasonal displacements for gravity trends, we get velocity as the immediate Earth's elastic response to the secularly changing surface load), and suggest the existence of slow uplift of tectonic and/or GIA origin.

An important question is how much part of the 2–3 mm yr^{-1} uplift comes from GIA. Kaufmann (2005) predicted current velocity and gravity changes assuming the large-GIA models (actually the small-GIA model does not predict measurable changes). The TIBET-4, one of the three large-GIA models, predicts 2–4 mm yr^{-1} uplift of Lhasa (Kaufmann, 2005), in agreement with the GPS results. If this is true, the uplift would be due entirely to GIA, i.e. we need to correct GRACE results. Fig. 4b shows gravity increase predicted by TIBET-4, after applying the 400 km Gaussian spatial filter. By subtracting these changes from GRACE observations, we get a revised estimate of
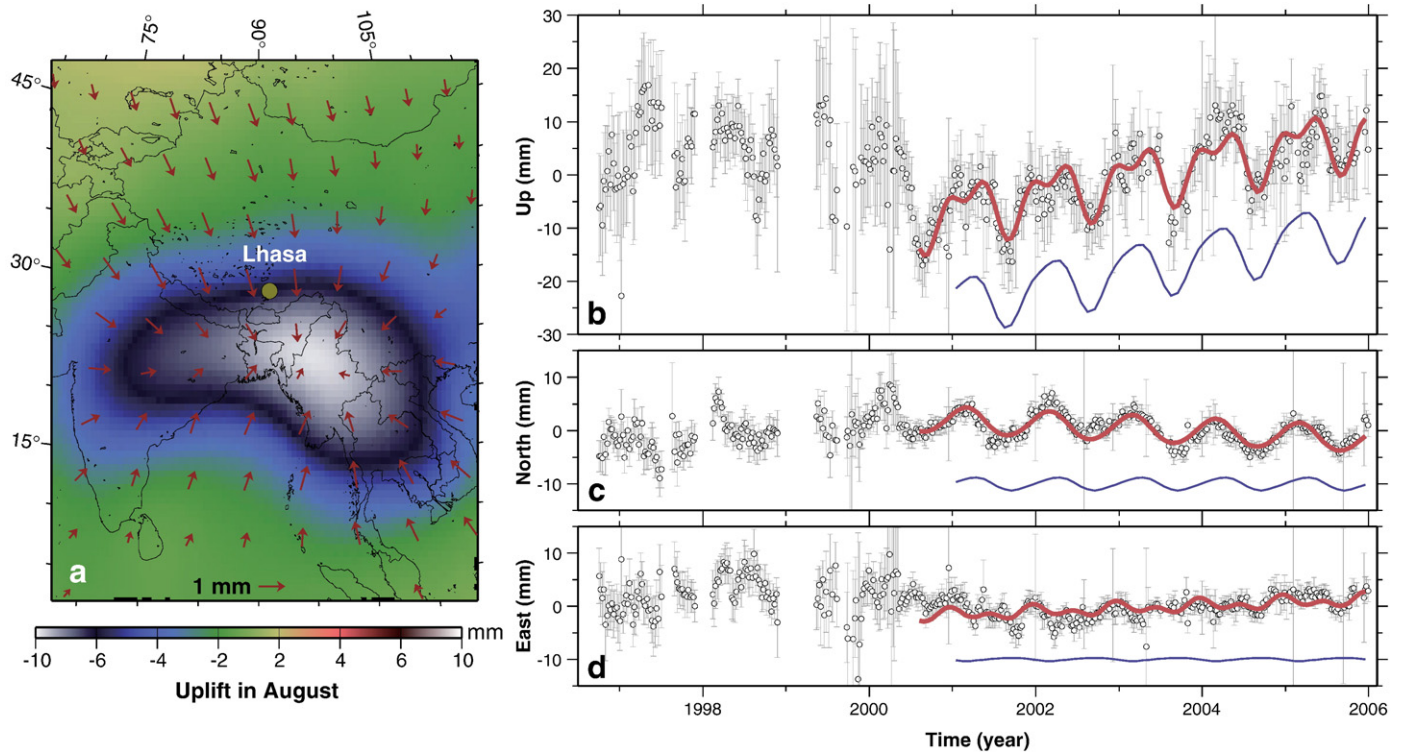

Fig. 6. Vertical and horizontal displacement at grid points due to surface load in August (average of 2002–2009) inferred from seasonal gravity change by GRACE (a). Residual time series of the Lhasa GPS station in ITRF2005 (Altamimi et al., 2007) in up (b), north (c), and east (d) components, show clear seasonal variations (red curves) consistent with those converted from seasonal gravity changes (blue curves, trends are arbitrary) only after ~2000.5 (amplitudes of the semi-annual components do not agree well due to unknown reasons). The data after 2000.5 show that Lhasa is uplifting by ~3 mm yr^{-1}. (For interpretation of the references to colour in this figure legend, the reader is referred to the web version of this article.)

$61\,\mathrm{Gt\,yr^{-1}}$ as the ice loss rate in HM Asia (red dot in Fig. 2). By substituting the other two large-GIA models (KUHLE and TIBET-6) given in Kaufmann (2005) for TIBET-4, this value changes by $+2$ and $-3\,\mathrm{Gt\,yr^{-1}}$, respectively (this uncertainty has been added to the error bar of the red dot in Fig. 2). On the other hand, the uplift of Lhasa might be entirely of tectonic origin because of its proximity to the Himalayas. In this case, we do not need correction and the estimated ice loss remains $47\,\mathrm{Gt\,yr^{-1}}$.

At the moment, there are no firm field observations supporting past large ice sheet on the Tibetan Plateau. In order to further constrain the ice loss rate in HM Asia, we need a continuous GPS network in Tibet dense enough to clarify ongoing tectonic/GIA uplifts. In this article, we will not further pursue this issue, and simply give both values in Fig. 2.

Ground gravimetry would also provide independent constraint on the process going on in Tibet. Sun et al. (2009) recently reported secular gravity decrease of $\sim 2.4\,\mu\mathrm{Gal\,yr^{-1}}$ at Lhasa with repeated absolute gravimetry, and attributed it partly to the subsidence of Moho of $\sim 2\,\mathrm{cm\,yr^{-1}}$. This is too fast even if the observed uplift is due entirely to crustal thickening, and the glacial melting might be largely responsible for the observed excess gravity decrease (they took account of crustal uplift but not glacial mass loss).

3.3. Glacial ice loss and sea level rise

The $47\,\mathrm{Gt\,yr^{-1}}$ ice loss in HM Asia is equivalent to $0.13\,\mathrm{mm\,yr^{-1}}$ sea level rise. If we extrapolate the linear relationship in Fig. 2 to the seasonal volume change of all the mountain glaciers in the world ($\sim 661\,\mathrm{km^3}$) (Meier, 1984), we obtain $264 \pm 36\,\mathrm{Gt\,yr^{-1}}$ as their total rate of loss (the error reflects the standard deviation of the estimated ratio between the two quantities), equivalent to $0.73 \pm 0.10\,\mathrm{mm\,yr^{-1}}$ sea level rise. This is similar to the value inferred for 1993–2003 by Intergovernmental Panel on Climate Change (Bindoff et al., 2007).

One important result of this work is that glacial mass losses are fairly variable in time and space (Fig. 4), i.e. mass balance of particular glacial regions might be influenced by decadal scale climatic fluctuations and differences in local responses to such fluctuations. Thus the estimation of ice loss rates in mountain glaciers and continental ice sheets should be repeated in various time windows to correctly understand long-term behavior of cryosphere in the warming Earth.

4. Conclusions

Here we conclude as follows;

(1) GRACE satellite gravimetry during 2003–2009 suggests that $47 \pm 12\,\mathrm{Gt\,yr^{-1}}$ glacial mass loss occurs in HM Asia.
(2) Possibility of GIA in the Tibetan Plateau cannot be ruled out, and the ice loss estimate could be revised upward to $61 \pm 13\,\mathrm{Gt\,yr^{-1}}$ by taking it into account.
(3) Accelerated melting of mountain glaciers worldwide might be contributing to the global sea level rise by $0.73 \pm 0.10\,\mathrm{mm\,yr^{-1}}$.
(4) Ice loss signature in HM Asia is highly variable in time and space.

Studying glacial losses in HM Asia is important in social aspect; numbers of major rivers flow out of this region and they may suffer shortage in dry season water flux in future (e.g. Barnett et al., 2005). For the assessment of long-term sustainability of Asian agriculture, we should keep investigating glacial mass balance there.

Appendix A. Supplementary data

Supplementary data associated with this article can be found, in the online version, at doi:10.1016/j.epsl.2009.11.053.

References

Ahmed, I., Umar, R., 2008. Hydrogeological framework and water balance studies in parts of Krishni–Yamuna interstream area, Western Uttar Pradesh, India. Environ. Geol. 53, 1723–1730.
Altamimi, Z., Collilieux, X., Legrand, J., Garayt, B., Boucher, C., 2007. ITRF2005: a new release of the International Terrestrial Reference Frame based on time series of station positions and Earth orientation parameters. J. Geophys. Res. 112, B09041. doi:10.1029/2007JB004949.
Amano, K., Taira, A., 1992. Two-phase uplift of higher Himalayas since 17 Ma. Geology 20, 391–394.
Arendt, A.A., Echelmeyer, K.A., Harrison, W.D., Lingle, C.S., Valentine, V.B., 2002. Rapid wastage of Alaska Glaciers and their contribution to rising sea level. Science 297, 383–386.
Bamber, J.L., Krabill, W., Raper, V., Dowdeswell, J.A., Oerlemans, J., 2005. Elevation changes measured on Svalbard glaciers and ice caps from airborne laser data. Ann. Glaciology 42, 202–208.
Barnett, T.P., Adam, J.C., Lettenmaier, D.P., 2005. Potential impacts of a warming climate on water availability in snow-dominated regions. Nature 438, 303–309.
Bettinelli, P., et al., 2006. Plate motion of India and interseismic strain in the Nepal Himalaya from GPS and DORIS measurements. J. Geod. 80, 567–589.
Bindoff, N.L., et al., 2007. Climate Change 2007: The Physical Science Basis. Contribution of Working Group I to the Fourth Assessment Report of the Intergovernmental Panel on Climate Change. Cambridge Univ. Press, New York. Chap.5.
Burbank, D.W., Leland, J., Fielding, E., Anderson, R.S., Brozovic, N., Reid, M.R., Duncan, C., 1996. Bedrock incision, rock uplift and threshold hillslopes in the northwestern Himalayas. Nature 379, 505–510.
Chao, B.F., 2005. On inversion for mass distribution from global (time-variable) gravity field. J. Geodynamics 39, 223–230.
Chen, J.L., Tapley, B.D., Wilson, C.R., 2006. Alaskan mountain glacial melting observed by satellite gravimetry. Earth Planet. Sci. Lett. 248, 368–378.
Chen, J.L., Wilson, C.R., Tapley, B.D., Blankenship, D.D., Ivins, E.R., 2007. Patagonia Icefield melting observed by Gravity Recovery and Climate Experiment (GRACE). Geophys. Res. Lett. 34, L22501. doi:10.1029/2007GL031871.
Cheng, M., Tapley, B.D., 2004. Variations in the Earth's oblateness during the past 28 years. J. Geophys. Res. 109, B09402. doi:10.1029/2004JB003028.
Davis, J.L., Eloségui, P., Mitrovica, J.X., Tamisiea, M.E., 2004. Climate-driven deformation of the solid Earth from GRACE and GPS. Geophys. Res. Lett. 31, L24605. doi:10.1029/2004GL021435.
Dyurgerov, M., Meier, M.F., 2005. Glaciers and the Changing Earth System: A 2004 Snapshot. Occasional Paper 58, Institute of Arctic and Alpine Research. University of Colorado, Boulder, p. 118.
Fujita, K., Ageta, Y., 2000. Effect of summer accumulation on glacier mass balance on the Tibetan Plateau revealed by mass-balance model. J. Glaciology 46, 244–252.
Heki, K., 2001. Seasonal modulation of interseismic strain buildup in Northeastern Japan driven by snow loads. Science 293, 89–92.
Hewitt, K., 2005. The Karakoram anomaly? Glacier expansion and the 'Elevation Effect, Karakoram Himalaya'. Mountain Res. Development 25, 332–340.
Jiménez-Munt, I., Fernàndez, M., Vergés, J.J., Platt, P., 2008. Lithospheric structure underneath the Tibetan Plateau inferred from elevation, gravity and geoid anomalies. Earth Planet. Sci. Lett. 267, 276–289.
Kaser, G., Cogley, J.G., Dyurgerov, M.B., Meier, M.F., Ohmura, A., 2006. Mass balance of glaciers and ice caps: consensus estimates for 1961–1994. Geophys. Res. Lett. 33, L19501. doi:10.1029/2006GL027511.
Kaufmann, G., 2005. Geodetic signatures of a Late Pleistocene Tibetan ice sheet. J. Geodyn. 39, 111–125.
Kaufmann, G., Lambeck, K., 1997. Implications of Late Pleistocene glaciations of the Tibetan Plateau for present-day uplift rates and gravity anomalies. Quat. Res. 48, 269–279.
Meier, M.F., 1984. Contribution of small glaciers to global sea level. Science 226, 1418–1421.
Meier, M.F., et al., 2007. Glaciers dominate eustatic sea-level rise in the 21st century. Science 317, 1064–1067.
Qiu, J., 2008. The third pole. Nature 454, 393–396.
Rignot, E., Rivera, A., Casassa, G., 2003. Contribution of the Patagonia icefields of South America to sea level rise. Science 302, 434–437.
Rodell, M., Velicogna, I., Famiglietti, J.S., 2009. Satellite-based estimates of groundwater depletion in India. Nature 460, 999–1002.
Rodell, M., et al., 2004. The global land data assimilation system. Bull. Amer. Meteor. Soc. 85, 381–394.
Rowley, D.B., Currie, B.S., 2006. Palaeo-altimetry of the Late Eocene to Miocene Lunpola basin, central Tibet. Nature 439, 677–681.
Singh, D.K., Singh, A.K., 2002. Groundwater situation in India: problems and perspectives. Water Resour. Dev. 18, 563–580.
Spicer, R.A., et al., 2003. Constant elevation of southern Tibet over the past 15 million years. Nature 421, 622–624.
Sun, W., et al., 2009. Gravity and GPS measurements reveal mass loss beneath the Tibetan Plateau — geodetic evidence of increasing crustal thickness. Geophys. Res. Lett. 36, L02303. doi:10.1029/2008GL036512.
Swenson, S.C., Wahr, J., 2006. Post-processing removal of correlated errors in GRACE data. Geophys. Res. Lett. 33, L08402. doi:10.1029/2005GL025285.

Tamisiea, M.E., Leuliette, E.W., Davis, J.L., Mitrovica, J.X., 2005. Constraining hydrological and cryospheric mass flux in southeastern Alaska using space-based gravity measurements. Geophys. Res. Lett. 32, L20501. doi:10.1029/2005GL023961.

Tamisiea, M.E., Mitrovica, J.X., Davis, J.L., 2007. Grace gravity data constrain ancient ice geometries and continental dynamics over Laurentia. Science 316, 881–883.

Tiwari, V.M., Wahr, J., Swenson, S., 2009. Dwindling groundwater resources in northern India, from satellite gravity observations. Geophys. Res. Lett. 36, L18401. doi:10.1029/2009GL039401.

Wahr, J., Molenaar, M., Bryan, F., 1998. Time variability of the Earth's gravity field: hydrological and oceanic effects and their possible detection using GRACE. J. Geophys. Res. 103, 30205–30229.

Wang, H., 2001. Effects of glacial isostatic adjustment since the Late Pleistocene on the uplift of the Tibetan Plateau. Geophys. J. Int. 144, 448–458.

Wang, Q., et al., 2001. Present-day crustal deformation in China constrained by global positioning system measurements. Science 294, 574–577.

Xu, C., Liu, J., Song, C., Jiang, W., Shi, C., 2000. GPS measurements of present-day uplift in the Southern Tibet. Earth Planets Space 52, 735–739.